

Loss Parameter Identification After Cutting for Different Non-Oriented Electrical Steel Grades

Nora Leuning¹, Benedikt Schauerte¹, Sebastian Schweren, and Kay Hameyer

Institute of Electrical Machines (IEM), RWTH Aachen University, 52063 Aachen, Germany

The magnetic properties of nonoriented (NO) electrical steel sheet are sensitive to industrial cutting processes. Decreased operation point efficiency and an increase in local iron loss in the magnetic circuit of an electrical machine are the consequences. During the design of electrical machines, the cut-edge effect and its consequences can only be considered and assessed, if the effect is locally modeled. In fact, the cut-edge effect is often neglected as standardized magnetic characterization is performed, where the sheet material is measured on an Epstein frame or single sheet tester (SST) and gentle sample preparation is specified. In order to parameterize a local material model, a large number of samples and their detailed magnetic characterization at various magnetizing frequencies are necessary. In this article, the loss parameters of nine different industrial NO electrical steels are identified and analyzed in order to study the course of the parameters and possible interrelation with material properties. The sheet thickness, alloying content of silicon and aluminum, and grain sizes are considered as they are the dominant influences on the iron loss from the material side. The presented results help to increase the understanding of the cut-edge effect and its consequences on the iron loss modeling. Furthermore, they help to identify possibilities to decrease the measurement effort significantly.

Index Terms—Cut-edge effect, electrical steel, iron loss modeling, magnetic properties.

I. INTRODUCTION

CUTTING of nonoriented (NO) electrical steel sheets has a significant effect on the magnetic properties: iron loss is increased and the magnetizability is decreased. The deterioration of the magnetic properties due to different cutting techniques and processing parameters has been studied for many years [1]–[4]. Spark erosion, chemical cutting, and abrasive water jet cutting are considered gentle methods, whereas punching and laser cutting are more detrimental [5], [6]. For mechanical cutting, small cutting clearance, new and sharp tools, and lower cutting speed lead to less deterioration [1]. As the deterioration is related to the plastic deformation and induced mechanical respective thermal residual stress, all measures which decrease the residual stress, decrease the influence of the cut-edge effect.

In addition to the cutting technique, the material properties, e.g., grain size, sheet thickness, and alloying, have an effect on the resulting deterioration as well [7]–[9]. As both, the residual stress and plastic deformation that cause the deterioration are induced in the vicinity of the cut edge, the effect appears locally. In [10], a review on the local distribution of the cut-edge effect is presented that summarizes the extent of the penetration depths of various studies.

Although the global effect of cutting can be measured on a single sheet tester (SST), an Epstein frame, or ring core samples with the approach presented in [4], the quantification and interpretation from global measurements to local information are more complicated [11]. Consequently, the incorporation of the cut edge in the design and calculation of electrical machines is challenging. The main requirement is to model

the magnetic properties locally. A continuous local material model is presented in [12], where the permeability is modeled with respect to the distance to the cut edge. The model is parameterized with modified SST samples. The local flux density can thereby be calculated with respect to the cut-edge effect in the finite-element simulation of any electrical machine geometry. The iron loss is subsequently calculated in the post-processing. Thus, the iron loss modeling has to be performed locally as well. The acquisition of data for the parameterization of a local iron loss model is cumbersome. A large number of cut material samples have to be characterized over a broad excitation range to account, for example, for high-efficient speed-variable traction drives with quasi-static frequencies up to several kHz. If the effect of cutting is better understood, fewer measurements for the parameterization and fewer samples are required. Furthermore, a material property-based estimation of the severity of the cut-edge effect for different NO can be enabled.

For this purpose, nine industrial electrical steels, which are mechanically cut, are analyzed and discussed in this article. Their loss parameters are identified to allow the analysis of the general course of the parameters with respect to an increasing proportion of cut edge of the entire volume. At the same time, the interrelation of loss parameters and the dominant material properties, i.e., grain size, sheet thickness, and alloying, is evaluated. It is shown that the iron loss parameters follow certain trends that allow a reduction of the number of samples without losing a significant amount of information.

II. MATERIALS AND METHODS

A. Materials

In this article, nine fully finished industrial NO electrical steels are studied. The sheet thickness, d_{sheet} , varies between 0.1 and 0.35 mm. In Table I, a summary of the nomenclature for the samples and their relevant material properties is given.

Manuscript received 28 October 2021; revised 3 February 2022; accepted 10 February 2022. Date of publication 15 February 2022; date of current version 26 July 2022. Corresponding author: N. Leuning (e-mail: nora.leuning@iem.rwth-aachen.de).

Color versions of one or more figures in this article are available at <https://doi.org/10.1109/TMAG.2022.3151844>.

Digital Object Identifier 10.1109/TMAG.2022.3151844

0018-9464 © 2022 IEEE. Personal use is permitted, but republication/redistribution requires IEEE permission. See <https://www.ieee.org/publications/rights/index.html> for more information.

TABLE I
NOMENCLATURE FOR THE STUDIED SAMPLES AND RESPECTIVE
RELEVANT MATERIAL PROPERTIES

Name	Grade	Si + Al in wt. %	d_{sheet} in mm	d_{GS} in μm
NO35-A	M235-35A	4.08	0.35	130
NO35-B	M235-35A	4.17	0.35	114
NO30	NO30-16	4.42	0.30	98
NO27-A	NO27-13	4.38	0.27	118
NO27-B	NO27-13	4.90	0.27	134
NO24	NO24-13	4.51	0.23	110
NO23	NO23-13	4.77	0.23	116
NO20	NO20-12	4.66	0.20	95
NO10	NO10-11	4.22	0.10	79

The alloying content has been obtained by spark spectrometry. The grain size, d_{GS} , has been evaluated on surface sections with the line intercept method in different layers of the steel sheet. Samples were evaluated on a light optical microscope. More than 300 grains were measured in each layer to account for a mean grain size value with respect to the layers.

B. Magnetic Measurements

Magnetic measurements are carried out on a 120 mm \times 120 mm SST (Brockhaus Measurements) on a MPG200. In order to quantify the cut-edge effect on an SST, samples are prepared according to [1] and [4]. The proportion of cut edge per sample is increased by dividing the reference sample size of 120 mm \times 120 mm into strips with an equal strip width, d_{strip} (Fig. 1.). In this study, d_{strip} were 120, 60, 30, 15, 10, 7.5, 5, and 4 mm. No stress relief annealing was carried out on the strips to maintain the fundamental cut-edge effect for the subsequent quantification. The strips are taped together to build up one SST sample of reference size with increasing shares of cutting-affected sample volume. In actual electrical machines, the deterioration of performance due to the cutting of the steel laminations can be separated into the fundamental cut-edge effect based on the induced stress and into the secondary effect of additional eddy currents, if burrs are large enough to connect the originally electrically isolated laminations of the electrical sheet stack. Possible burrs at the cut edges due to the wear state of the cutting tool do not affect the measurements of this study on the fundamental cut-edge effect, as measurements are carried out on SST. For testing in RD and TD, separate sample sets are prepared, as to prevent an air gap in the magnetic flux path, i.e., cutting direction is parallel to the applied magnetic field. The samples were all cut mechanically on a guillotine, which is similar to the process of punching, used in mass series production. The cutting method and parameters were kept the same for all materials during this study. In Fig. 1, a schematic description of the SST setup is presented. Measurements are carried out up to a magnetizing frequency of 5000 Hz between 0.1 and 1.8 T in 0.1 T steps under sinusoidal excitation.

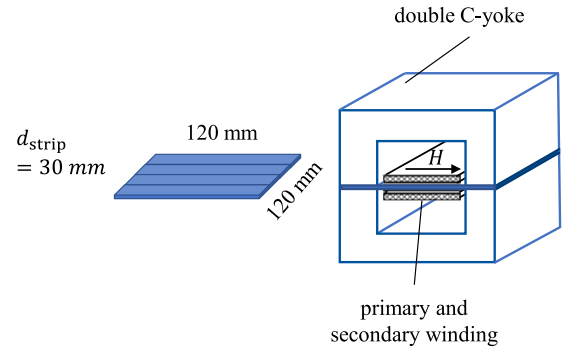


Fig. 1. Schematic description of the sample preparation and measurement of the cut-edge samples on an SST.

C. Loss Model Parameter Identification

In order to incorporate the cut-edge effect and subsequent consideration of local iron loss in an electrical machine, a continuous local material model embedded in a numerical finite-element (FE) simulation environment has to be applied. Each FE is attributed a material property according to the distance x to the nearest cut edge. The procedure is described in detail in [12]. For the evaluation of local iron loss in the post-processing of an electrical machine simulation, the loss has to be modeled as a function of the distance to the cut edge as well [13]. In order to do so, the loss parameters have to be identified.

The IEM-Formula is a semi-physical loss model that allows a physical interpretation of different loss components [14]. Such an interpretation enables the detailed evaluation of the relationship between the machine design, machine operation, and utilized electrical steel. The IEM-Formula is based on the loss separation principle [15]. The total iron loss is separated into a hysteresis, classical eddy current, and excess component similar to Bertotti's approach [15], but is complemented by a fourth higher order loss term. This loss represents nonlinear or saturation. The resulting IEM-Formula is as follows:

$$P_{\text{IEM}} = a_1 B_m^{\alpha+\beta} f + a_2 B_m^2 f^2 (1 + a_3 B_m^{a_4}) + a_5 (B_m f)^{1.5}. \quad (1)$$

The identification process of parameters, a_i , α , and β , as described in [16], is based on the statistical loss theory. The hysteresis parameters, a_1 , α , and β , can be fitted from low-frequency measurements. The classical eddy current component, a_2 , is calculated based on the sheet thickness, d_{sheet} , specific density, ρ , and specific electrical resistivity, ρ_{el}

$$a_2 = \frac{\pi^2 d_{\text{sheet}}^2}{6\rho\rho_{\text{el}}}. \quad (2)$$

The excess loss parameter, a_5 , can either be identified by measurements at relatively low magnetic flux densities up to 1.0 T and frequencies between below 10 Hz or calculated solely from material-dependent properties based on the theory of magnetic objects. The parameters a_3 and a_4 are mathematically determined from the magnetic characteristic at high frequencies and magnetic flux densities. Thus, all iron loss terms of the IEM-Formula (1) are identified.

III. RESULTS AND DISCUSSION

A. Results of the Parameter Identification Routine

For this study, more than 100 material samples have been magnetically characterized on an SST and their loss parameters have been identified as described in Section II. Each sample set of the nine studied materials comprises eight samples with different strip widths between 120 and 4 mm. All electrical steels have a full sample set with cut directions parallel to the rolling direction (RD) of the steel sheet. An additional six out of the nine studied materials have been studied on a sample set in the transverse direction (TD) as well.

In Fig. 2, the identified parameters for $a_1 a_5$ are presented for all samples in RD with the exception of a_2 parameter as it is independent of the strip width, d_{strip} , according to (2). In general, all parameters follow a distinct trend. The parameters a_1 , a_3 , and a_5 all increase with decreasing strip width; a_4 , on the other hand, increases. For all parameters, the increase and decrease are especially pronounced at narrow strip widths below 10 mm and keeps almost constant between 30 and 120 mm strip widths. Considering the physical interpretation of the loss components of the IEM-Formula, this is the expected behavior. The hysteresis loss is the static loss component that is related to the domain wall movement and Barkhausen jumps. The domain wall movement is impeded by defects such as grain boundaries or in this case by dislocation structures or shear bands at the cut edge. Furthermore, the domain wall movement is strongly impeded by mechanical stress, which leads to an increase in loss, especially for compressive stress [17], [18]. Residual mechanical stress that is part compressive, part tensile [1], and remains in the vicinity of the cut edge after cutting, strongly affects the hysteresis loss and thereby the course of a_1 . In [17]–[19], it is presented that mechanical stress has a negative effect on the excess loss component as well. In general, compressive stress is more detrimental compared with tensile stress.

The trends are not equally distinct for all the studied sample sets. Some identified parameters are obvious statistical outliers, for example in Fig. 2(d), the NO20, 60 mm sample, whereas some materials are more prone to statistical errors in general. Especially, the very thin NO10 and NO20 electrical steels show a scattering of their parameters.

To evaluate outliers and in order to decrease the measurement effort significantly, the course of the parameters can be depicted alternatively. In Fig. 3, a_1 is shown over the ratio of cut surface per sample volume, δ_{strip} . A linear regression fits the general curve of the parameters. The linear fit is characterized by the slope of the curve and the y-axis intercept. Both these parameters show a link to the material parameters as shown in Fig. 4. The slope of the linear regression generally decreases with decreasing sheet thickness, increasing alloying content and to a minor extent with decreasing grain size. The Y-intercept decreases slightly with increasing sheet thickness, increasing alloying and grain size. As these parameters all influence the hysteresis loss to some extent, it is impossible to fully separate the effect of each single parameter in these industrial NO electrical steel sheets. In general, thinner materials have smaller overall grain sizes, so these parameters

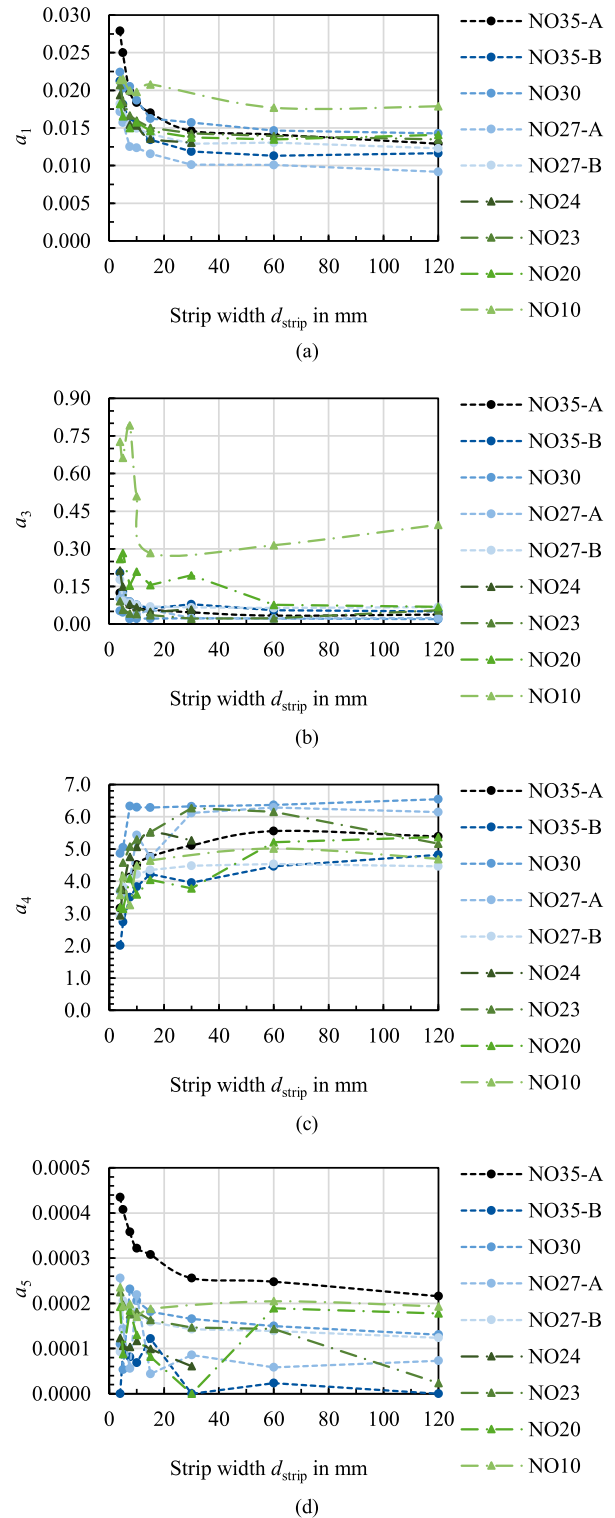


Fig. 2. Identified loss parameters as a function of strip width, d_{strip} , for all studied materials in RD. (a) Hysteresis loss parameters. (b) and (c) Nonlinear loss parameters. (d) Excess loss parameters.

are linked as well. But the examples show that the linear regression is not only mathematically a good fit, but can also be physically interpreted, which is important for the semi-physical loss modeling approach. Furthermore, the linear regression is not only valid for the samples in RD as depicted, but also for the sample sets in TD. In direct comparison,

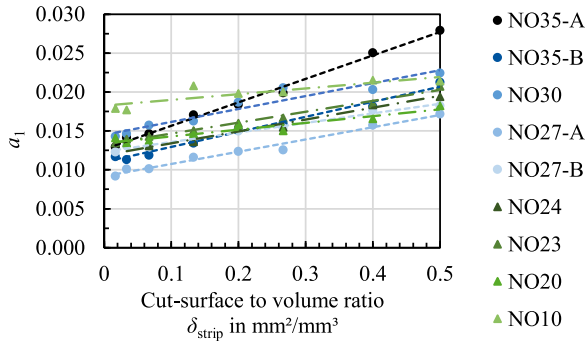


Fig. 3. Hysteresis loss parameter a_1 as a function of cut-surface ratio per sample volume with linear regression.

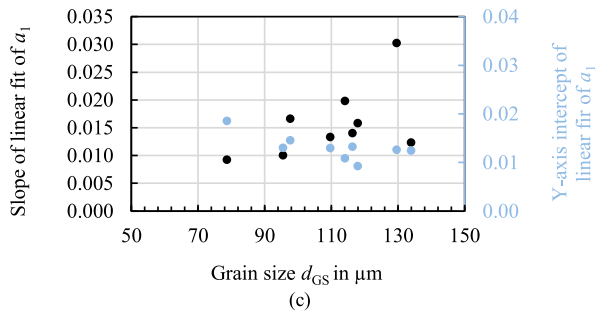
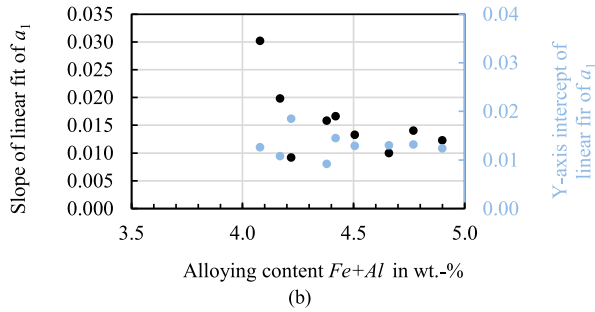
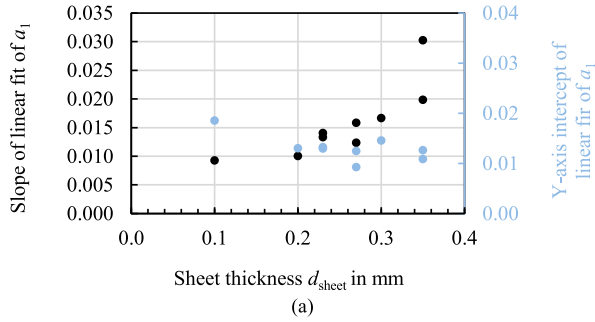


Fig. 4. Correlation between the linear regression parameters and material parameters: (a) sheet thickness, (b) alloying content, and (c) grain size.

a_1 is higher in TD compared with RD for all respective sample sets.

B. Utilization of Results to Reduce Sample Number

The hysteresis coefficient is not the only parameter that has a distinct course over the cut surface per sample volume ratio. In Fig. 5, the courses of a_3 , a_4 , and a_5 are shown. In Fig. 5(a), the two thinnest materials are not shown, as they breached the scale of the diagram. This shows that not every parameter course follows the trend. This is likely due to the standardized

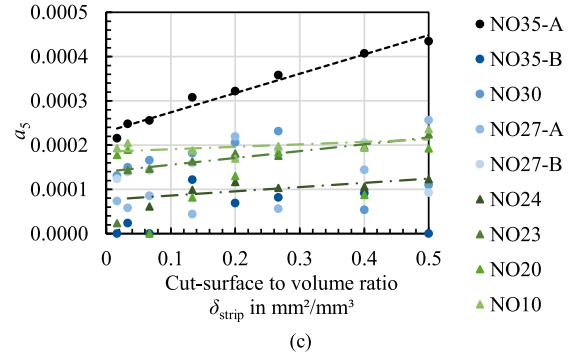
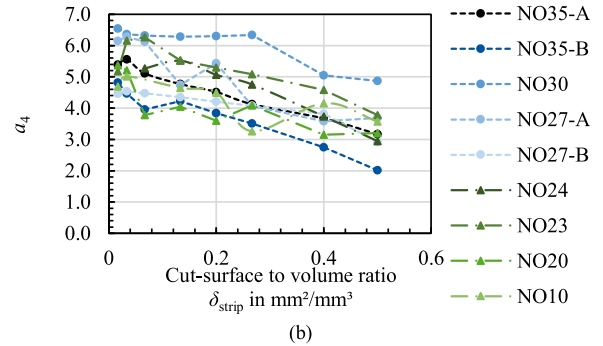
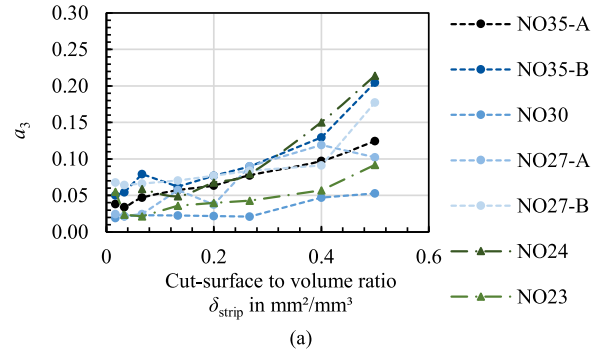


Fig. 5. Identified loss parameters as a function of cut-surface ratio. (a) and (b) Nonlinear loss parameters. (c) Excess loss parameters.

identification routine and could be improved by a variation of frequencies considered to identify the nonlinear and excess loss components.

Due to the analysis of the parameter courses and the generally similar trends for all materials, a significant reduction of the sample number can be enabled. For this part of the study, the sample number reduced by 50%. Instead of eight samples per sample set, only four samples were evaluated. The parameter courses, i.e., a linear regression of a_1 , a_4 , and a_5 and an exponential function of a_3 were deduced from the parameters of only the 120, 30, 7.5, and 5 mm samples. The results are shown in Fig. 6 and compared to the measured values of all strip widths. There are higher discrepancies for a_4 in the range between 10 and 30 mm, but overall the results are promising.

It can be seen that this procedure does not downgrade the quality of the results more than the statistical errors shown in Fig. 2. With only half of the measurement required, a sufficient amount of information for the loss modeling can be obtained. Although the risk of an increased impact of statistical errors

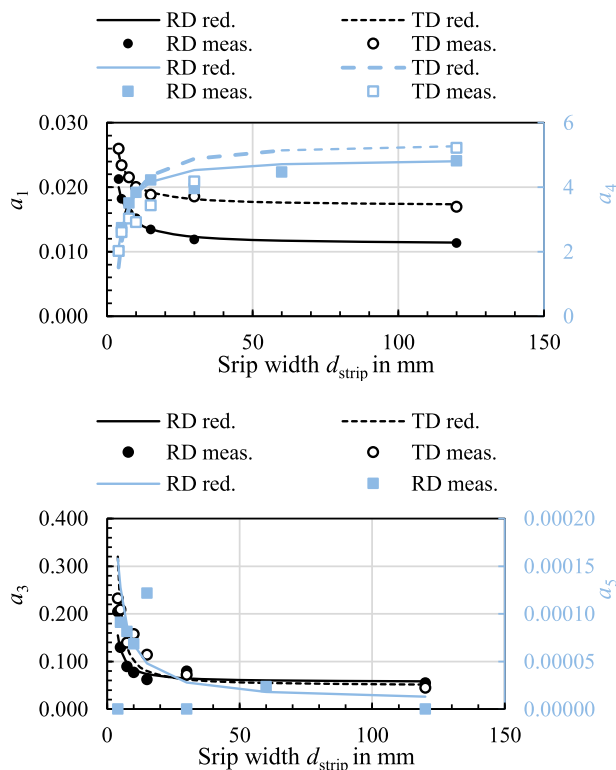


Fig. 6. Comparison of loss parameters as a function of strip width, d_{strip} , with a decreased sample set size (red) for NO35B in RD and TD.

on the identification has to be considered, the reduced measurement effort is significant. A larger material selection could be considered during a simulation study, as these parameters are essential for the local modeling of loss as a function of distance.

IV. CONCLUSION

In this article, the effect of cut edges on loss parameters of electrical steel sheets has been studied. The results were obtained by analyzing the course of the loss parameters as a function of an increasing portion of cut edge on nine different industrial electrical steels and conclusion can be summarized as follows:

- 1) The analysis of the loss parameters allows a linear regression (a_1 , a_3 , and a_5) and adapted exponential regression (a_4) for the different loss parameters.
- 2) It was shown that the sample number and experimental characterization effort can thereby be significantly reduced.
- 3) The results and physical interpretation of the hysteresis and excess loss component are in accordance with the results presented in this article, i.e., sensitivity of the hysteresis loss to cutting increases with increasing sample thickness, decreasing alloy content and increasing grain size for electrical steels in this thickness range.

ACKNOWLEDGMENT

This work was supported by the German Research Foundation (DFG) through research groups FOR1897 under Grant 255713208 and SPP2013 under Grant HA 4395/22-1.

REFERENCES

- [1] H. A. Weiss *et al.*, "Influence of shear cutting parameters on the electromagnetic properties of non-oriented electrical steel sheets," *J. Magn. Magn. Mater.*, vol. 421, pp. 250–259, Jan. 2017, doi: [10.1016/j.jmmm.2016.08.002](https://doi.org/10.1016/j.jmmm.2016.08.002).
- [2] R. Siebert, J. Schneider, and E. Beyer, "Laser cutting and mechanical cutting of electrical steels and its effect on the magnetic properties," *IEEE Trans. Magn.*, vol. 50, no. 4, pp. 1–4, Apr. 2014, doi: [10.1109/TMAG.2013.2285256](https://doi.org/10.1109/TMAG.2013.2285256).
- [3] H. M. S. Harstick, M. Ritter, A. Plath, and W. Riehemann, "EBSD investigations on cutting edges of non-oriented electrical steel," *Metallography, Microstruct., Anal.*, vol. 3, no. 4, pp. 244–251, Aug. 2014, doi: [10.1007/s13632-014-0148-2](https://doi.org/10.1007/s13632-014-0148-2).
- [4] A. Schoppa, J. Schneider, and J.-O. Roth, "Influence of the cutting process on the magnetic properties of non-oriented electrical steels," *J. Magn. Magn. Mater.*, vols. 215–216, pp. 100–102, Jun. 2000, doi: [10.1016/S0304-8853\(00\)00077-9](https://doi.org/10.1016/S0304-8853(00)00077-9).
- [5] A. Schoppa, H. Louis, F. Pude, and C. von Rad, "Influence of abrasive waterjet cutting on the magnetic properties of non-oriented electrical steels," *J. Magn. Magn. Mater.*, vols. 254–255, pp. 370–372, Jan. 2003, doi: [10.1016/S0304-8853\(02\)00882-X](https://doi.org/10.1016/S0304-8853(02)00882-X).
- [6] M. Emura, F. Landgraf, W. Ross, and J. Barreta, "The influence of cutting technique on the magnetic properties of electrical steels," *J. Magn. Magn. Mater.*, vols. 254–255, pp. 358–360, Jan. 2003, doi: [10.1016/S0304-8853\(02\)00856-9](https://doi.org/10.1016/S0304-8853(02)00856-9).
- [7] R. Rygal, A. Moses, N. Derebasi, J. Schneider, and A. Schoppa, "Influence of cutting stress on magnetic field and flux density distribution in non-oriented electrical steels," *J. Magn. Magn. Mater.*, vols. 215–216, pp. 687–689, Jun. 2000, doi: [10.1016/S0304-8853\(00\)00259-6](https://doi.org/10.1016/S0304-8853(00)00259-6).
- [8] N. Leuning, S. Steentjes, and K. Hameyer, "Impact of grain size distribution on the magnetic deterioration due to cutting of electrical steel sheets," *J. Magn. Magn. Mater.*, vol. 497, Mar. 2020, Art. no. 166080, doi: [10.1016/j.jmmm.2019.166080](https://doi.org/10.1016/j.jmmm.2019.166080).
- [9] H. A. Weiss *et al.*, "Neutron grating interferometry investigation of punching-related local magnetic property deteriorations in electrical steels," *J. Magn. Magn. Mater.*, vol. 474, pp. 643–653, Mar. 2019, doi: [10.1016/j.jmmm.2018.10.098](https://doi.org/10.1016/j.jmmm.2018.10.098).
- [10] M. Bali and A. Muetze, "The degradation depth of non-grain oriented electrical steel sheets of electric machines due to mechanical and laser cutting: A state-of-the-art review," *IEEE Trans. Ind. Appl.*, vol. 55, no. 1, pp. 366–375, Jan. 2019, doi: [10.1109/TIA.2018.2868033](https://doi.org/10.1109/TIA.2018.2868033).
- [11] T. P. Holopainen, P. Rasilo, and A. Arkkio, "Identification of magnetic properties for cutting edge of electrical steel sheets," *IEEE Trans. Ind. Appl.*, vol. 53, no. 2, pp. 1049–1053, Mar./Apr. 2017, doi: [10.1109/TIA.2016.2638405](https://doi.org/10.1109/TIA.2016.2638405).
- [12] S. Elfgen, S. Steentjes, S. Bohmer, D. Franck, and K. Hameyer, "Continuous local material model for cut edge effects in soft magnetic materials," *IEEE Trans. Magn.*, vol. 52, no. 5, pp. 1–4, May 2016, doi: [10.1109/TMAG.2015.2511451](https://doi.org/10.1109/TMAG.2015.2511451).
- [13] B. Groschup, S. Elfgen, and K. Hameyer, "Iron loss simulation using a local material model," *COMPEL Int. J. Comput. Math. Electr. Electron. Eng.*, vol. 38, no. 4, pp. 1224–1234, Jul. 2019, doi: [10.1108/COMPEL-10-2018-0421](https://doi.org/10.1108/COMPEL-10-2018-0421).
- [14] D. Eggers, S. Steentjes, and K. Hameyer, "Advanced iron-loss estimation for nonlinear material behavior," *IEEE Trans. Magn.*, vol. 48, no. 11, pp. 3021–3024, Nov. 2012, doi: [10.1109/TMAG.2012.2208944](https://doi.org/10.1109/TMAG.2012.2208944).
- [15] G. Bertotti, "General properties of power losses in soft ferromagnetic materials," *IEEE Trans. Magn.*, vol. MAG-24, no. 1, pp. 621–630, Jan. 1988.
- [16] S. Steentjes, M. Leßmann, and K. Hameyer, "Semi-physical parameter identification for an iron-loss formula allowing loss-separation," *J. Appl. Phys.*, vol. 113, no. 17, May 2013, Art. no. 17A319, doi: [10.1063/1.4795618](https://doi.org/10.1063/1.4795618).
- [17] A. P. S. Baghel, J. B. Blumenfeld, L. Santandrea, G. Krebs, and L. Daniel, "Effect of mechanical stress on different core loss components along orthogonal directions in electrical steels," *Elect. Eng.*, vol. 101, pp. 845–853, Sep. 2019, doi: [10.1007/s00202-019-00827-4](https://doi.org/10.1007/s00202-019-00827-4).
- [18] D. Singh, P. Rasilo, F. Martin, A. Belahcen, and A. Arkkio, "Effect of mechanical stress on excess loss of electrical steel sheets," *IEEE Trans. Magn.*, vol. 51, no. 11, pp. 1–4, Nov. 2015, doi: [10.1109/TMAG.2015.2449779](https://doi.org/10.1109/TMAG.2015.2449779).
- [19] J. Karthaus, S. Elfgen, N. Leuning, and K. Hameyer, "Iron loss components dependent on mechanical compressive and tensile stress in non-oriented electrical steel," *Int. J. Appl. Electromagn. Mech.*, vol. 59, no. 1, pp. 255–261, Mar. 2019, doi: [10.3233/JAE-171020](https://doi.org/10.3233/JAE-171020).